



# Effects of anode layer linear ion source on the microstructure and mechanical properties of amorphous carbon nitride films



Peng Ye<sup>a</sup>, Feng Xu<sup>a,\*</sup>, Jinxin Wu<sup>a</sup>, Shuai Tian<sup>a</sup>, Xianrui Zhao<sup>a,b</sup>, Xiaolong Tang<sup>a</sup>, Dunwen Zuo<sup>a,\*</sup>

<sup>a</sup> College of Mechanical and Electrical Engineering, Nanjing University of Aeronautics and Astronautics, Nanjing 210016, China

<sup>b</sup> College of Physics and Electronic Engineering, Zhejiang Provincial Key Laboratory for Cutting Tools, Taizhou University, Taizhou 318000, China

## ARTICLE INFO

### Article history:

Received 10 August 2016

Revised 13 January 2017

Accepted in revised form 17 January 2017

Available online 18 January 2017

### Keywords:

Anode layer linear ion source

Amorphous carbon nitride films

RFMS

Microstructure

Mechanical properties

## ABSTRACT

In order to study the effects of anode layer linear ion source (ALLIS) on the microstructure and mechanical properties of amorphous carbon nitride ( $a\text{-CN}_x$ ) films,  $a\text{-CN}_x$  films were deposited by the ALLIS assisted radio frequency magnetron sputtering (RFMS) deposition condition changing the ion source power from 0 to 200 W. The growth rate, structural morphology, surface roughness, nanohardness as well as the bonding states of deposited  $a\text{-CN}_x$  films were characterized by scanning electron microscope (SEM), atomic force microscope (AFM), nano-indentation, Raman spectroscopy and X-ray photoelectron spectroscopy (XPS), respectively. The  $H/E$  and hardness increased relatively with increasing the ion source power up to 100 W. From the Micro Raman analysis, the content of  $\text{sp}^3$  carbon in  $\text{sp}^3/\text{sp}^2$  ratio was increased with increasing the ion source power. The cross-sectional SEM images demonstrated that the ion source enhanced the growth rate of  $a\text{-CN}_x$  films. Meanwhile, the roughness was increased with the ion source power above 100 W. Therefore, the optimum ion source power is considered to be around 100 W in these experimental conditions.

© 2017 Elsevier B.V. All rights reserved.

## 1. Introduction

Amorphous carbon nitride ( $a\text{-CN}_x$ ) films are structurally analogous diamond-like materials. On account of the high atom density and strong covalent bonds, both of them have prominent physical and chemical properties, such as extreme hardness, outstanding thermal conductivity, high chemical stability, great biocompatibility, good corrosion resistance and excellent wear and friction properties [1,2]. The composition and structure of  $a\text{-CN}_x$  films are very complex, and the properties of films prepared by different preparation methods and technologies are distinguishing. Recently, significant progress in the synthesis of  $\text{CN}_x$  films has been made by various physical vapor deposition (PVD) and chemical vapor deposition (CVD) processes, such as the magnetron sputtering [3], pulsed laser deposition [4], ion beam deposition [5], plasma immersion ion implantation [6], filtered cathode arc [7], magnetron sputtering method [8] as well as plasma-enhanced chemical vapor deposition [9]. Nevertheless, it is still lack of in-depth understanding to deposition mechanism, process, microstructure and properties of  $a\text{-CN}_x$  films. Therefore, it is of practical significance to research the preparation technology and properties of  $a\text{-CN}_x$  films.

Magnetron sputtering is one of the preferred methods for the synthesis of carbon based amorphous materials such as boron carbides

( $\text{B}_4\text{C}$ ), diamond-like carbon (DLC) and  $\text{CN}_x$  because of its effective dissociation of nitrogen molecule, simple scalability and easy control of deposition conditions [10]. Broitman et al. [11] studied the tribological properties of  $a\text{-CN}_x$  films prepared at different substrate temperature and nitrogen partial pressure, and found that the film friction coefficients tended to increase for different substrates as the nitrogen content in the film was increased. Wei et al. [12] found that there existed an optimized nitrogen partial pressure where the nanohardness and the wear resistance of the film were the highest. Deposition parameters such as gas flux, substrate bias voltage, ion energy and ion density as well as substrate temperature in magnetron sputtering were also investigated by some researchers [11,12].

The low gas ionization rate has been a major challenge during the preparation of  $a\text{-CN}_x$  films in magnetron sputtering. In order to improve the ionization rate of gas, auxiliary ion sources such as additional Kaufman ion source [13], end-Hall ion source [14], ion beam [15] as well as anode layer linear ion source (ALLIS) [16,17] were applied to the deposition of films. Kim et al. [17] prepared the DLC films with ALLIS assisted physical vapor deposition, and found that suitable ion source voltage promoted the fraction of  $\text{sp}^3$  bonds in the DLC films. Qi Jun et al. [18] studied the effects of argon ion beam on the properties of DLC coatings using dual ion source system, and obtained the highest  $\text{sp}^3$ -hybridized carbon content of films synthesized with the Ar ion energy of 400 eV. Compared with other auxiliary ion sources, ALLIS is a relatively effective technology for depositing  $a\text{-CN}_x$  films. The main advantages of this technique are the low cost, simple structure and increase rate of gas

\* Corresponding authors at: College of Mechanical and Electrical Engineering, Nanjing University of Aeronautics and Astronautics, Nanjing 210016, China.

E-mail addresses: [xufeng@nuaa.edu.cn](mailto:xufeng@nuaa.edu.cn) (F. Xu), [zuodw@nuaa.edu.cn](mailto:zuodw@nuaa.edu.cn) (D. Zuo).

ionization. ALLIS in the magnetic field makes the electrons bound in the vicinity of the anode surface forming dense plasma region and gas ionize. A low energy, high flow ion beam produced can effectively remove organic pollutants and the oxidation layer on substrate surface, increase adhesion and avoid damage to the substrate during bombardment. To the best of our knowledge, the study on this kind of auxiliary ion source deposition of  $a\text{-CN}_x$  films has not been reported.

In present study, a variety of  $a\text{-CN}_x$  films were successfully deposited on the silicon substrate at ion source powers ranging from 0 to 200 W by ALLIS assisted magnetron sputtering method. The influences of ALLIS on the microstructure and bonding configuration of carbon and nitrogen atoms in  $a\text{-CN}_x$  films were investigated systematically by Raman spectrum and X-ray photoelectron spectroscopy (XPS). Finally, the growth rate, nanomechanical properties of deposited  $a\text{-CN}_x$  films were characterized by scanning electron microscopy (SEM) and nano-indentation tests, respectively.

## 2. Experimental

Amorphous carbon nitrogen ( $a\text{-CN}_x$ ) films were deposited by radio frequency magnetron sputtering (RFMS, JSD450-III) at a frequency of 13.56 MHz using anode layer linear ion source (ALLIS). The schematic diagrams of the experimental apparatus and ALLIS are shown in Fig. 1a–b. The target material was a 5 mm thick disk made of pyrolytic graphite with a purity of 99.999%. The direct current component of the substrate potential was referred to the substrate bias voltage. In order to produce denser plasma near the substrate surface and increase the flux density of impinging ions, ALLIS was installed between the target and substrate holder, as shown in Fig. 1a.

Due to the high requirement of the PVD method for the cleanliness of the equipment, the vacuum chamber should be cleaned enough before each experiment, and then the substrate was placed in the vacuum chamber. High-purity single-sided polishing p-type (100) silicon wafer was cut to  $1.0 \times 1.0 \text{ cm}^2$  substrates. The silicon substrates were immersed into 10% concentration of HF solution for 10 min to wipe off the oxide on its surface and then ultrasonically cleaned, in proper order, in acetone, methanol and deionized water for 10 min to remove the surface contaminants, finally dried in a flow of dry nitrogen. Prior to deposition, the substrates were outgassed at  $400^\circ\text{C}$  in high vacuum for 30 min, and then sputter-cleaned in an Ar discharge with a negative bias of 200 V for 20 min. The magnetron target was pre-sputtered with a closed shutter at 90 W for 10 min. ALLIS is a type of ion generator which can be introduced into various gases. A gas mixture of nitrogen and argon which passed through the slit was ionized and charged particles were accelerated electrostatically. During film deposition, the frequency

**Table 1**  
Deposition parameters of  $a\text{-CN}_x$  films.

Parameters	Values
Total gas flow rate (sccm)	40
Base pressure (Pa)	$5 \times 10^{-4}$
RF power (W)	250
Anode layer linear ion source power (W)	0–200
Target-to-substrate distance (mm)	90
Substrate temperature ( $^\circ\text{C}$ )	150
Substrate bias voltage (V)	–50
Working gas pressure (Pa)	0.5
$\text{N}_2$ content in the sputtering gas (%)	50
Deposition time (min)	60

and duty cycle of ALLIS with defocusing discharge mode (low voltage, high current, high duty cycle) were kept at 38 kHz and 50%. The ion source power was varied from 0 to 200 W (Table 1). The other control factors were fixed.

For the characterization, the microstructure of the samples was analyzed using a LABRAM-HR800 Raman spectrometer with excitation wavelength of 514.5 nm. The chemical composition and bonding states of the carbon and nitrogen atoms on the surface of  $a\text{-CN}_x$  films were characterized using a PERKIN-ELMER CHI 5300 X-ray photoelectron spectroscopy (XPS) with Al-K $\alpha$  radiation line (1486.6 eV). The samples surface was etched by Ar ion for 10 min conducted to remove contamination prior to XPS analysis. XPSPEAK software was used fitting the C1s and N1s core level spectra in XPS. Shirley function was modeled as the backgrounds. The surface structure and roughness of deposited samples were characterized by Atomic force microscope (AFM) from CSPM 3000, which operated in contact mode with scan area at  $1.2 \times 1.2 \mu\text{m}^2$ . The growth rate of a sample was calculated by dividing its thickness by corresponding deposition duration. The cross-sections of the specimens were studied by scanning electron microscopy (SEM, Hitachi-S4800). The hardness ( $H$ ) and elastic modulus ( $E$ ) were measured by nano-indentation (Agilent technologies, G-200) tests using continuous stiffness method (CSM).

## 3. Results and discussion

### 3.1. Microstructure

The influence of ion source power on the Raman spectra of  $a\text{-CN}_x$  films and deconvoluted Raman spectrum of the  $a\text{-CN}_x$  film deposited at an ion source power of 100 W are investigated in Fig. 2a. The curves were displaced vertically for clarity. These spectra of  $a\text{-CN}_x$  films are

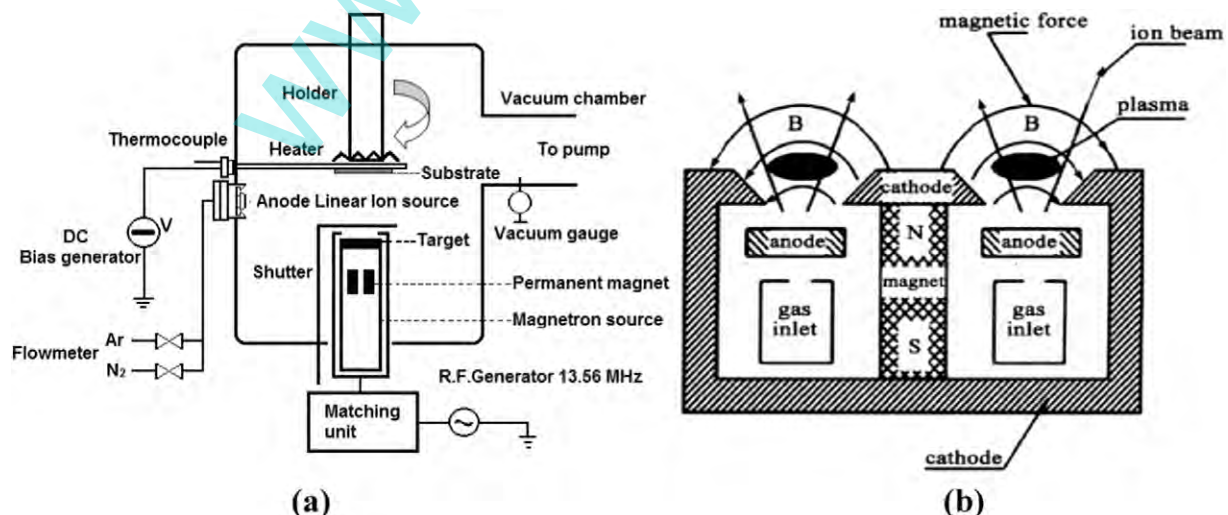


**Fig. 1.** Schematic diagrams of (a) ALLIS assisted RFMS system and (b) ALLIS.

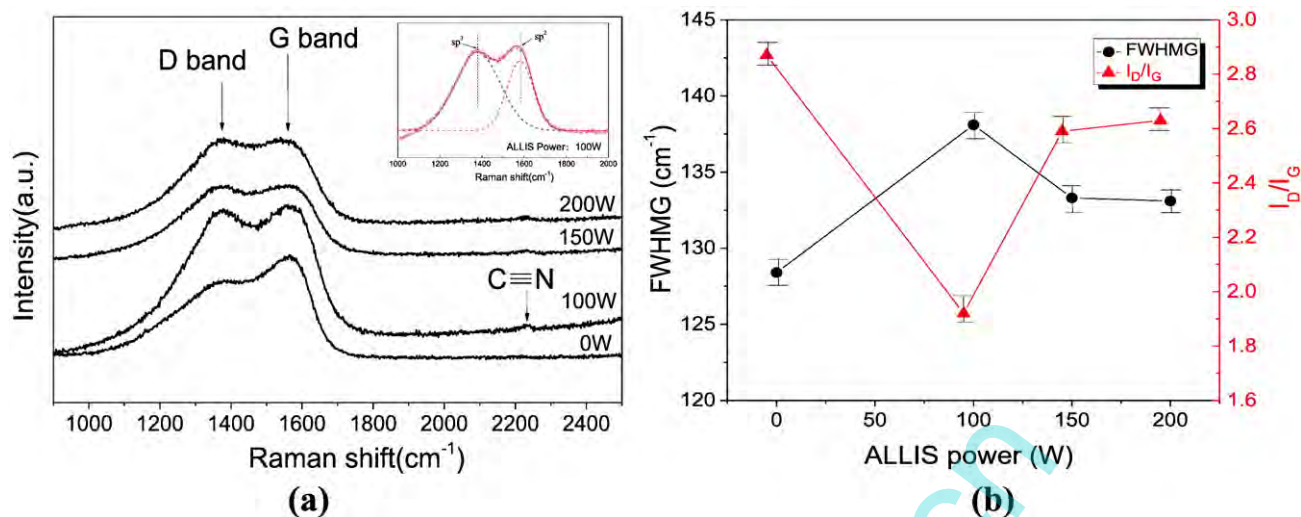


**Fig. 2.** (a) Raman spectra of  $\alpha\text{-CN}_x$  films on Si for various ion source powers and the deconvolution of Raman peaks of  $\alpha\text{-CN}_x$  (100 W) films and (b) the FWHM of G peak (FWHMG), the intensity ratio of D to G peak ( $I_D/I_G$ ) variations with the ion source power for deposited samples.

practically consistent with the corresponding spectrum of the diamond like carbon film. The intensities and widths of G and D bands of the samples located at approximately 1550 and 1360  $\text{cm}^{-1}$  changed obviously at different ion source powers. The weakest D peak observed as  $\alpha\text{-CN}_x$  films were deposited at 100 W. With further increasing ion source power from 100 to 200 W, the peak position of G mildly shifts toward the high frequencies and the D peak becomes more intense. The width and intensity of D band are related to the lattice disorder induced by N incorporation and the nitrogen ion bombardment in  $\alpha\text{-CN}_x$  films [19, 20]. Beside the typical carbon D and G bands, other additional bands were also observed after the ion source was used. The band observed at approximately 2200  $\text{cm}^{-1}$ , can be associated with nitrile radicals (C≡N bond) [20]. The Raman spectra of samples were deconvoluted into two Gaussian bands, which were D band and G band. The D band arises from the breathing modes of  $\text{sp}^2$  carbon atoms in clusters of six-fold rings. The G band originates from the bond-stretching modes of  $\text{sp}^2$  carbon atoms in both six-fold rings and chains [21]. Fig. 2b shows the full width at half maximum of G band (FWHMG), and the intensity ratio of D to G peaks ( $I_D/I_G$ ) as a function of ion source power.

According to Raman analysis, the synthesized films in this work were  $\alpha\text{-CN}_x$ , which contained a mixture of  $\pi$  and  $\sigma$  bonding [20]. Since Raman scattering from  $\pi$  bonds is 50–230 times stronger than that from  $\sigma$  bonds [22], the D and G modes caused by  $\pi$  bonding dominated the Raman spectra of deposited films. The positions of the G peaks were in the range of 1552–1571  $\text{cm}^{-1}$ , lower than graphite (1580  $\text{cm}^{-1}$ ), which was due to bond angle distortions and other disorders [22]. The FWHMG is related to the bond angle distortions in the excited

configurations, and low value of FWHMG corresponds to high ordered  $\text{sp}^2$  configurations [16]. The variation of  $I_D/I_G$  ratio with increasing ion source power showed a different trend with the FWHMG. Usually, high content of  $\text{sp}^2$  carbon clusters corresponds to high  $I_D/I_G$  ratio [22, 23]. Accordingly, the content of  $\text{sp}^2$  carbon clusters decreased with ion source power up to 100 W, however, further increasing ion source power resulted in the  $\text{sp}^3$  structure transforming to graphite structure. The ionization rate of gas and gas reaction activity increased with the increasing of ion source power. In the surface layer of materials, incident ions caused ‘thermal spike’ which instantaneously induced high temperature and high pressure in a rather limited area, promoting the formation of  $\text{sp}^3$  configuration [24]. Meanwhile, over high ion bombarding energy causes the  $\text{sp}^3$  transforming into  $\text{sp}^2$  configuration, which is possibly due to the thermally activated diffusion [24–26]. In addition, since Raman spectra is sensitive to  $\text{sp}^2$  hybridization and insensitive to  $\text{sp}^3$  hybridization, the real  $\text{sp}^2$  fraction in  $\alpha\text{-CN}_x$  films is lower than that suggested by experimental  $I_D/I_G$  ratio [27].

For deeply investigating the bonding states of  $\alpha\text{-CN}_x$  films, the C1s and N1s high resolution XPS spectra were decomposed, as presented in Fig. 3. The C1s spectra of deposited films contained four well-resolved peaks (denoted by C1s-1, C1s-2, C1s-3 and C1s-4) with a FWHM about 1.6 eV in the range of 284–289 eV (Fig. 3a). The peak C1s-1 corresponds to  $\text{sp}^2$  carbon bonding, and the peak C1s-2 is assigned to  $\text{sp}^3$  carbon bonding [28,29]. The peak C1s-3 and C1s-4 correspond to carbon multiple bonding with nitrogen [28,30] and carbon bonding with oxygen caused by foreign impurity in the films [31], respectively. The N1s spectra contained four main components with a FWHM about 1.5 eV, as

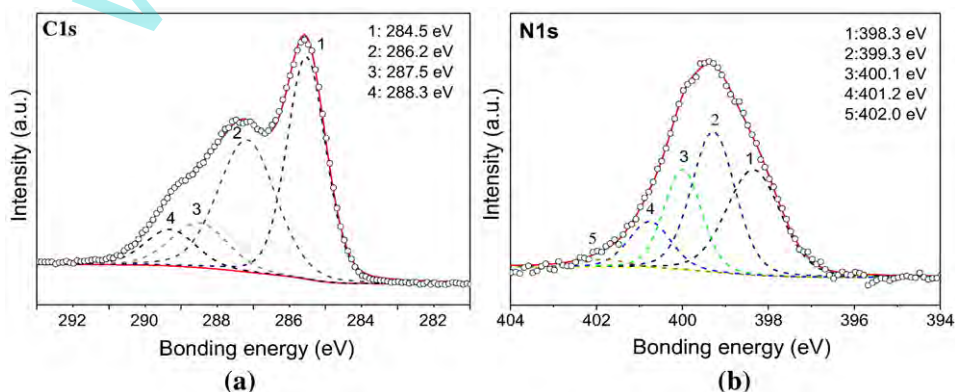


**Fig. 3.** XPS high resolution spectra of the  $\alpha\text{-CN}_x$  (100 W) film (a) C1s and (b) N1s.



shown in Fig. 3b. The five peaks (denoted by N1s-1, N1s-2, N1s-3, N1s-4 and N1s-5) were at the binding energy of 398.3, 399.3, 400.1, 401.2 and 402.0 eV, respectively. Peaks N1s-1, N1s-2, N1s-3 and N1s-4 correspond to N—C, N≡C, N=C and N=N (N<sub>2</sub>) bonds, respectively [23]. Peak N1s-5 is likely to be non-polar nitrogen molecule bond [31].

XPS spectra can be not only used for the qualitative determination of the elements of the *a*-CN<sub>x</sub> film, but also be used for quantitative determination of the elements. The N/C ratio of the deposited *a*-CN<sub>x</sub> films can be determined from the ratio of integrated net intensities of the N1s (A<sub>N</sub>) to C1s lines (A<sub>C</sub>) in the XPS spectra of deposited films by using

$$\frac{n_N}{n_C} = [(A_N/0.5)/(A_C/0.31)]$$

where the constants of 0.51 and 0.31 are the atomic sensitivity factors of nitrogen and carbon, respectively [32].

The [N]/[C] and sp<sup>3</sup>/sp<sup>2</sup> carbon ratio of *a*-CN<sub>x</sub> films with different ion source powers are seen in Fig. 4, respectively. [N]/[C] ratio is an important factor influencing the microstructure of *a*-CN<sub>x</sub> films. It can be seen that the use of the ALLIS greatly increased nitrogen fraction and sp<sup>3</sup>/sp<sup>2</sup> in the films. The ratio of N/C in the film increased to a maximum of 0.55 at an ion source power of 100 W. However, a further increase in the ion source power would slightly decrease the N/C ratio in the films. When *a*-CN<sub>x</sub> films were deposited without the ion source, the carbon species interacted solely with the N<sub>2</sub> molecules in the ambient gas, and a lower incorporation of N atoms in the film occurs. When ALLIS was used during the film deposition, the carbon species would interact with reactive nitrogen atoms and N<sup>+</sup> ion supplied by the RF discharge. This would improve the incorporation of N atoms in the films. The amount of nitrogen in the films depends on their sticking probabilities and sputtering yield at the growing film surface [33]. However, with ion source power further increasing, the sputtering effect of N ions became stronger, the carbon atoms on the film surface might lose their nitrogen neighbors due to preferential sputtering of nitrogen [34]. The kinetic energy of N ions partially translated into thermal energy when N ions impacted on film surfaces [35]. Sufficient thermal energy made film atoms to achieve more thermally activated mobility. Therefore the chemical reactions happened between incident N ions and the N atoms in CN species to form N≡N bonding. N escaped from the film in the style of nitrogen molecule, caused chemical re-sputtering. The chemical re-sputtering was thermally activated and was enhanced by increasing ion source power. That was the main reason for the decrease of nitrogen content in the films. The sp<sup>3</sup>/sp<sup>2</sup> ratio was calculated according to the ratio of C1s-1 to C1s-2 peak area. It was found that the variation of the sp<sup>3</sup>/sp<sup>2</sup> ratio had the similar trend with the [N]/[C] ratio. XPS

analysis indicated that increasing N content would increase sp<sup>2</sup> carbon and reduce sp<sup>3</sup> carbon in the films.

The three-dimensional AFM images of the samples are demonstrated in Fig. 5a–d. It can be seen that the surface micrograph of *a*-CN<sub>x</sub> films was obviously dependent on the ion source power. The surface of *a*-CN<sub>x</sub> (100 W) is relatively smooth without visible protuberance compared to other samples. With further increasing the ion source power, the film surface changed from smooth to a peak-and-valley structure, and the film surface became rougher. The rms values of the samples increased from 1.6 to 2.71 nm, and the rms value of *a*-CN<sub>x</sub> (100 W) was minimum (Fig. 5e). For compared, *a*-CN<sub>x</sub> (0 W) has the bigger roughness, this indicates that ALLIS has obvious influence on the film surface microtopography. ALLIS can effectively improve the nitrogen ionization rate, and increase ions bombarding energy. The ballistic effects of incident N<sup>+</sup> ions increased the mobility of film atoms, which resulted in downhill diffusion along the inclined surface, leading to the smoothness of the film surface [36]. On the contrary, sputtering effect was enhanced by increasing bombarding energy, induced film surface roughening.

In addition, cross-sectional SEM images were taken in order to study the effect of the ion source power on the growth rate of the *a*-CN<sub>x</sub> film. As shown in Fig. 6a–d, the thickness of samples increased from around 200 to around 300 nm with increasing the ion source power. This is because the number of high-energy ions increases with increasing ion source power, and therefore, the number of particles deposited on the substrate increases. The growth rate gradually increased from 3.3 to 5 nm/min (Fig. 6e), which indicated that ALLIS had obvious promoting effect on the deposition rate of *a*-CN<sub>x</sub> films.

### 3.2. Nanomechanical properties

Fig. 7a showed the *H* and *E* behavior as function of the indentation depth of representative *a*-CN<sub>x</sub> (100 W) sample. With the increased indentation depth, the hardness of deposited films also enhanced from nearly 0 to the maximum, and then followed by a slow downward trend (Fig. 7a). The nanohardness and [N—C]/[N≡C] of samples as function of ion source power are presented in Fig. 7b. The highest hardness observed as *a*-CN<sub>x</sub> films were deposited at an ion source power of 100 W. Compared with the case without ion source, nanohardness of deposited films had greatly promoted, this suggested that the ALLIS had an obvious effect to improve the nanohardness of the *a*-CN<sub>x</sub> film.

Additionally, Jing Ni et al. [37] suggested that [N—C]/[N≡C] ratio had a close relationship with the hardness of CN<sub>x</sub> films. Because the N≡C bond as terminating group breaks the continuity of the network in the structure of CN<sub>x</sub> films, high concentration of the N≡C bond makes the film structure less compact [21]. The decrease of [N—C]/[N≡C] ratio with increased ion source power above 100 W also contributes to the softened *a*-CN<sub>x</sub> films. The sp<sup>3</sup> content has great influences on the mechanical properties of *a*-CN<sub>x</sub> films, and high sp<sup>3</sup> content is accompanied by large hardness and elastic modulus. Raman spectra showed the sp<sup>3</sup> content of samples increased with increasing the ion source power, and then decreased with further increase in ion source power, the sp<sup>2</sup> content had opposite trend with that. The films transformed between the graphitization and cubic phase, thus hardness and elastic modulus were changing. Contrarily, sp<sup>2</sup> configuration not only contains weak π bonding, but also damages the connectivity of the covalent network, which leads the film softening. Therefore, increasing sp<sup>3</sup>/sp<sup>2</sup> carbon ratio improves the hardness of the film [38]. In this work, the high fraction of sp<sup>2</sup> bonding and low fraction of sp<sup>3</sup> bonding coexisted in *a*-CN<sub>x</sub> films as indicated in XPS results shown in Fig. 4. It was found that with increasing ion source power above 100 W, the sp<sup>3</sup>/sp<sup>2</sup> carbon ratio decreased from 0.51 to 0.43, so the hardness gradually decreased.

The variations of the *H/E* and *H<sup>3</sup>/E<sup>2</sup>* ratio of *a*-CN<sub>x</sub> films as a function of ion source power are investigated in Fig. 8. The ratio of the hardness to elastic modulus (*H/E*) of the film is the plastic index, which is an effective mean to explain the deformation mechanism of films, and it is also one of the indexes to predict the wear resistance of the material [39].

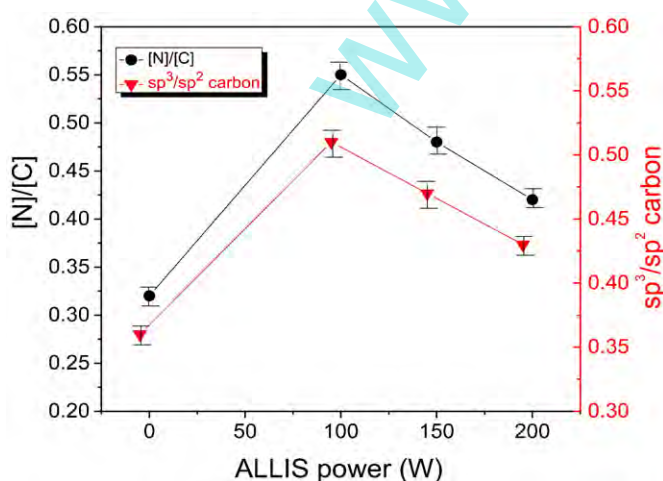
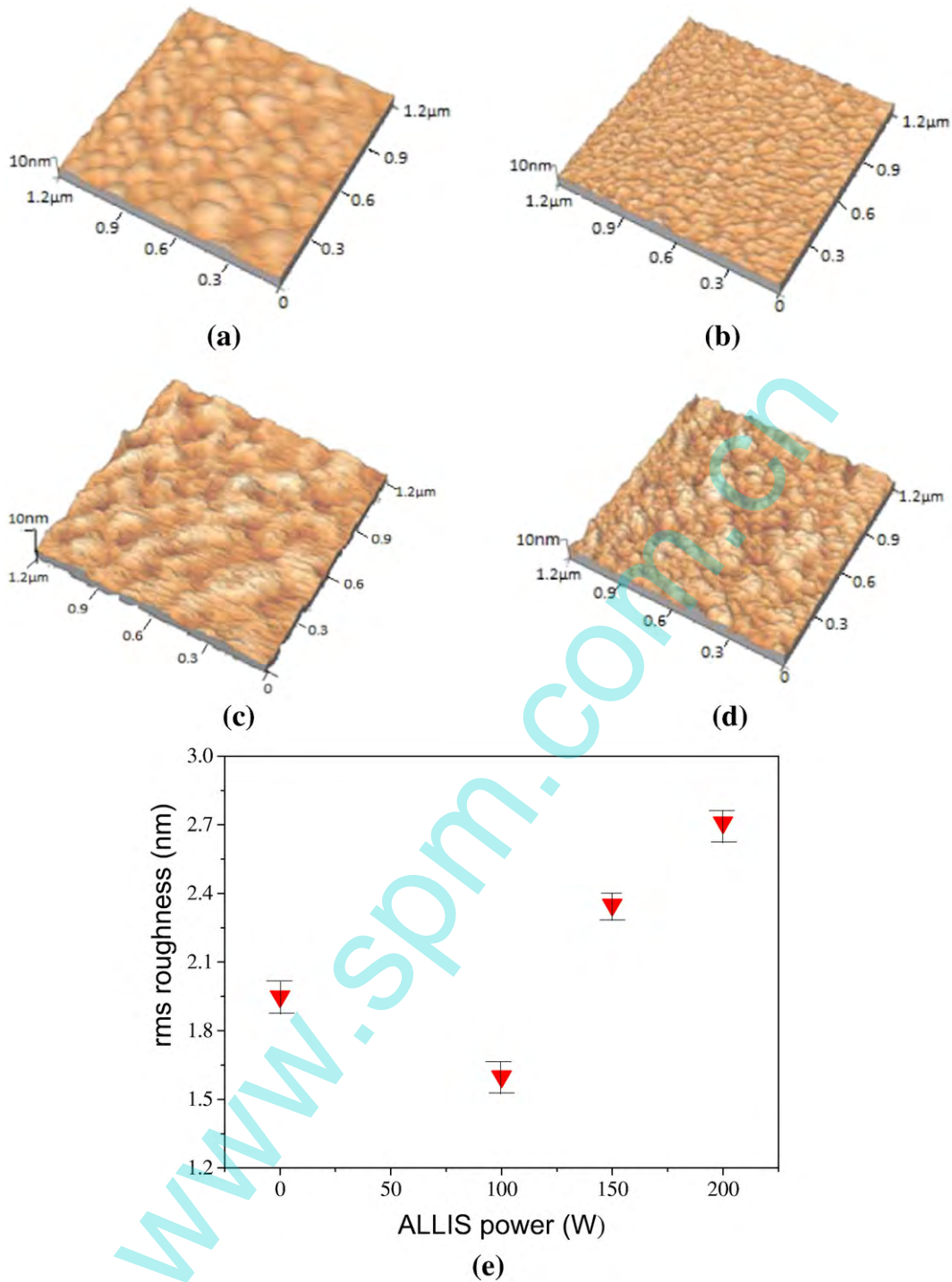


Fig. 4. [N]/[C] and sp<sup>3</sup>/sp<sup>2</sup> carbon ratio of *a*-CN<sub>x</sub> films as a function of ion source power.



**Fig. 5.** Three-dimensional AFM images of  $a\text{-CN}_x$  films with different ion source powers (a) 0 W, (b) 100 W, (c) 150 W, (d) 200 W, and (e) the root mean square (rms) roughness of  $a\text{-CN}_x$  films as function of ion source power.

The value of  $H/E$  varies between 0 (plastic behavior) and 0.1 (elastic behavior) for carbon coatings [40], and high value of  $H/E$  means that these films are highly resistant to plastic deformation [41]. The term  $H^3/E^2$  combines the  $H$  and  $E$  values of a material and sets the amount of the elasticity exhibited by the film. Particularly, high (low) values of  $H^3/E^2$  are correlated to the high elasticity (plasticity) deformation, and the greater values of  $H^3/E^2$  represent the better fracture toughness of the film [39]. The value of  $H/E$  without ALLIS was 0.098, while the value of the  $a\text{-CN}_x$  (100 W) film was promoted to 0.123, then dropped to 0.109 with the power increasing to 200 W. These results indicated appropriate ion source power was beneficial to the improvement of elasticity but

exorbitant ion source power made elasticity of the film decline. Values of  $H^3/E^2$  displayed the same trend with the ratio of  $H/E$  which illustrated the fracture toughness of films increased firstly and then decreased.

#### 4. Conclusions

By using anode layer linear ion source (ALLIS) assisted RFMS technology, amorphous carbon nitride ( $a\text{-CN}_x$ ) films were successfully prepared on the Si (100) substrate. The effects of ALLIS on the surface chemical bonding configuration and mechanical properties of  $a\text{-CN}_x$

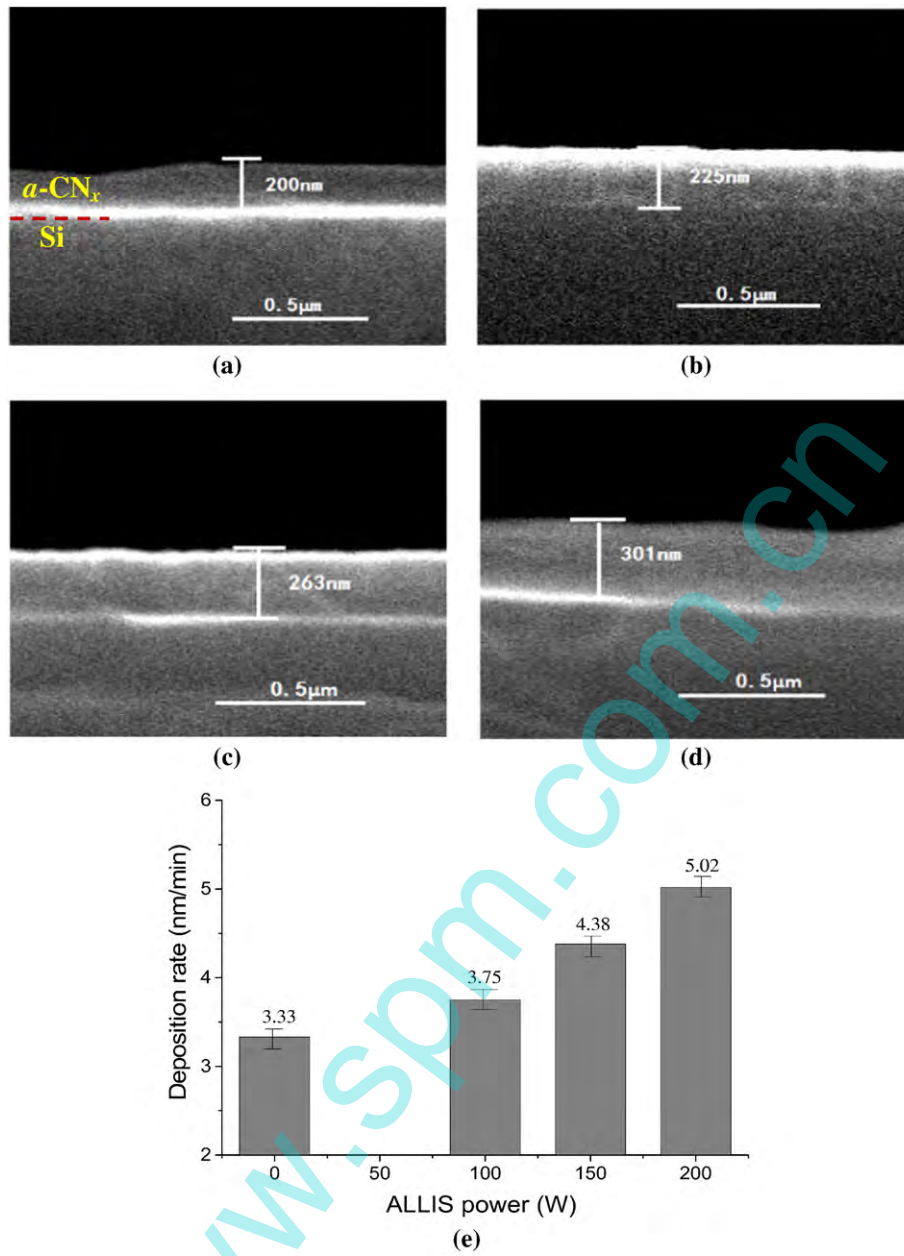


Fig. 6. The cross-sectional images of SEM in deposited  $\alpha$ -CN<sub>x</sub> films with different ion source powers (a) 0 W, (b) 100 W, (c) 150 W, (d) 200 W, and (e) the growth rate variations with the ion source power for deposited samples.

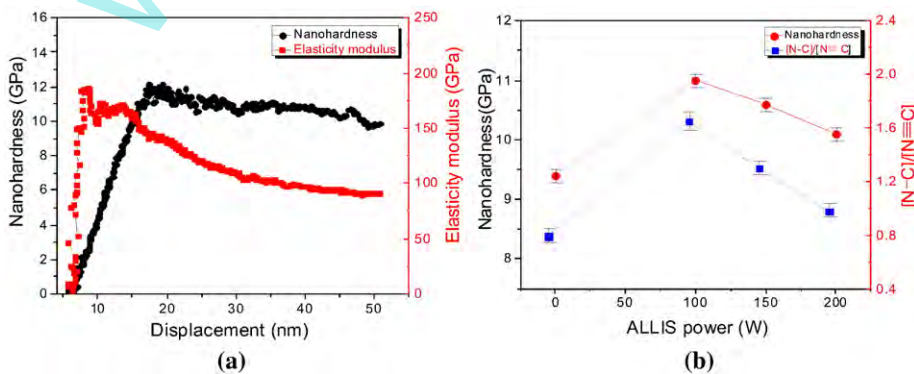


Fig. 7. (a) Nanohardness and elasticity modulus variations with the displacement for the  $\alpha$ -CN<sub>x</sub> (100 W) film and (b) nanohardness and [N-C]/[N=C] ratio of  $\alpha$ -CN<sub>x</sub> films as function of ion source power.



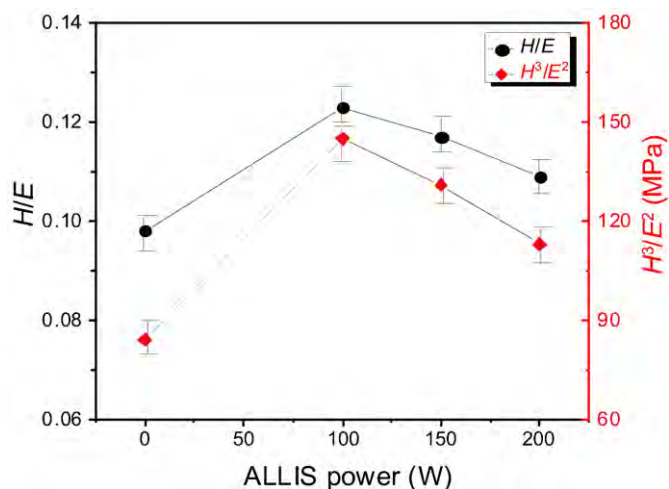


Fig. 8.  $H/E$  and  $H^3/E^2$  ratio variations with the ion source power for  $a\text{-CN}_x$  films.

films have been investigated systematically. The conclusions could be summarized as:

- (1) With an increase in ALLIS power, the deposition rate of films increased from 3.3 to 5 nm/min and surface quality had been significantly improved while the minimum surface roughness of  $a\text{-CN}_x$  films was obtained at an ion source power of 100 W in the range of experiment condition.
- (2) The existence of ALLIS effectively enhanced the  $sp^3$  carbon bond content and hardness of the film. Moreover, films prepared at an ion source power of 100 W presented maximum hardness, highest content of cubic phase and better fracture toughness. Thus ALLIS has played an enormous role in the improvement of mechanical properties of  $a\text{-CN}_x$  films.

### Acknowledgments

This work is supported by the National Natural Science Foundation of China (No. 51575269) and the Six Talent Peaks Project in Jiangsu Province of China (No. ZBZZ-005).

### References

- [1] S.E. Rodil, S. Muhl, Bonding in amorphous carbon nitride, *Diam. Relat. Mater.* 13 (2004) 1521–1531.
- [2] R.V. Shalaev, A.N. Ulyanov, A.M. Prudnikov, Noncatalytic synthesis of carbon-nitride nanocolumns by dc magnetron sputtering, *Phys. Status Solidi A* 207 (2010) 2300–2302.
- [3] E. Broitman, N. Hellgren, K. Järrendahl, Electrical and optical properties of  $\text{CN}_x$  ( $0 = x = 0.25$ ) films deposited by reactive magnetron sputtering, *J. Appl. Phys.* 89 (2001) 1184–1190.
- [4] F. Bourquard, C. Maddi, C. Donnet, A.S. Loir, Effect of nitrogen surrounding gas and plasma assistance on nitrogen incorporation in a-C: N films by femtosecond pulsed laser deposition, *Appl. Surf. Sci.* 374 (2016) 104–111.
- [5] B. Zhou, X. Jiang, A.V. Rogachev, R. Shen, D. Sun, A comparison study between atomic and ionic nitrogen doped carbon films prepared by ion beam assisted cathode arc deposition at various pulse frequencies, *Appl. Surf. Sci.* 287 (2013) 150–158.
- [6] S. Flege, R. Hatada, M. Hoefling, A. Hanauer, Modification of diamond-like carbon films by nitrogen incorporation via plasma immersion ion implantation, *Nucl. Inst. Methods Phys. Res. B* 365 (2015) 357–361.
- [7] H. Liang, C. Xian, Y. Li, W. Yanwu, W. Xiaoyan, Synthesis and structure of nitrogenated tetrahedral amorphous carbon films prepared by nitrogen ion bombardment, *Appl. Surf. Sci.* 257 (2011) 6945–6951.
- [8] I. Banerjee, N. Kumari, A.K. Singh, M. Kumar, P. Laha, Influence of RF power on the electrical and mechanical properties of nano-structured carbon nitride thin films deposited by RF magnetron sputtering, *Thin Solid Films* 518 (2010) 7240–7244.
- [9] M. Othman, R. Ritikos, N.H. Khanis, N.M.A. Rashid, Effects of rf power on the structural properties of carbon nitride thin films prepared by plasma enhanced chemical vapour deposition, *Thin Solid Films* 519 (2011) 4981–4986.
- [10] Y.S. Park, H.S. Myung, J.G. Han, B. Hong, Characterization of  $\text{CN}_x$  thin films prepared by close field unbalanced magnetron sputtering, *Thin Solid Films* 475 (2005) 298–302.
- [11] E. Broitman, N. Hellgren, O. Wänstrand, M.P. Johansson, Mechanical and tribological properties of  $\text{CN}_x$  films deposited by reactive magnetron sputtering, *Wear* 248 (2001) 55–64.
- [12] B. Wei, B. Zhang, K.E. Johnson, Nitrogen-induced modifications in microstructure and wear durability of ultrathin amorphous-carbon films, *J. Appl. Phys.* 83 (1998) 2491–2499.
- [13] H.R. Kaufman, J.J. Cuomo, J.M.E. Harper, Technology and applications of broad-beam ion sources used in sputtering. Part I. Ion source technology, *J. Vac. Sci. Technol.* 21 (1982) 725–736.
- [14] H.R. Kaufman, R.S. Robinson, End-Hall ion source, *J. Vac. Sci. Technol. A* 5 (1987) 2081–2084.
- [15] D.G. Liu, W.Q. Bai, Y.J. Pan, J.P. Tu, Crystalline carbon nitride film synthesized by ion beam assisted magnetron sputtering and thermal annealing in nitrogen gas, *Diam. Relat. Mater.* 55 (2015) 102–107.
- [16] S. Paskvale, M. Kahn, M. Čekada, P. Panjan, Tribological properties of diamond-like carbon coatings prepared by anode layer source and magnetron sputtering, *Surf. Coat. Technol.* 205 (2011) S99–S102.
- [17] W.R. Kim, M.S. Park, U.C. Jung, et al., Effect of voltage on diamond-like carbon thin film using linear ion source, *Surf. Coat. Technol.* 243 (2014) 15–19.
- [18] Q. Jun, L. Jianbin, W. Shizhu, et al., Mechanical and tribological properties of non-hydrogenated DLC films synthesized by IBAD, *Surf. Coat. Technol.* 128 (2000) 324–328.
- [19] J.H. Kaufman, S. Metin, D.D. Superstein, Symmetry breaking in nitrogen-doped amorphous carbon: infrared observation of the Raman-active G and D bands, *Phys. Rev. B* 39 (1989) 13053.
- [20] A. Chowdhury, D.C. Cameron, M.S.J. Hashmi, Vibrational properties of carbon nitride films by Raman spectroscopy, *Thin Solid Films* 332 (1998) 62–68.
- [21] G.J. Kovács, M. Veres, M. Koós, G. Radnóczy, Raman spectroscopic study of magnetron sputtered carbon-nickel and carbon nitride-nickel composite films: the effect of nickel on the atomic structure of the  $\text{C/CN}_x$  matrix, *Thin Solid Films* 516 (2008) 7910.
- [22] S.E. Rodil, A.C. Ferrari, J. Robertson, Raman and infrared modes of hydrogenated amorphous carbon nitride, *J. Appl. Phys.* 89 (2001) 5425–5430.
- [23] A.C. Ferrari, S.E. Rodil, J. Robertson, Interpretation of infrared and Raman spectra of amorphous carbon nitrides, *Phys. Rev. B* 67 (2003) 155306.
- [24] Y. Miyagawa, H. Nakadate, M. Tanaka, Dynamic MC simulation of DLC films synthesis by PBI, *Surf. Coat. Technol.* 156 (2002) 87–91.
- [25] S. Praver, K.W. Nugent, Y. Lifshitz, G.D. Lempert, Systematic variation of the Raman spectra of DLC films as a function of  $sp^2:sp^3$  composition, *Diam. Relat. Mater.* 5 (1996) 433–438.
- [26] J. Wang, W.Z. Li, Influence of the bombardment energy of  $\text{CH}_4^+$  ions on the properties of diamond-like carbon films, *Surf. Coat. Technol.* 122 (1999) 273–276.
- [27] H.S. Zhang, K. Komvopoulos, Direct-current cathodic vacuum arc system with magnetic-field mechanism for plasma stabilization, *Rev. Sci. Instrum.* 79 (2008), 073905.
- [28] Z.R. Wu, M. Zhang, F.Z. Cui, Adhesion and growth of smooth muscle cells on  $\text{CN}_x$  coatings, *Surf. Coat. Technol.* 201 (2007) 5710.
- [29] T. Ujvári, A. Kolitsch, A. Tóth, et al., XPS characterization of the composition and bonding states of elements in  $\text{CN}_x$  layers prepared by ion beam assisted deposition, *Diam. Relat. Mater.* 11 (2002) 1149.
- [30] B. Bouchet-Fabre, G. Lazar, D. Ballutaud, Influence on the  $sp^3/sp^2$  character of the carbon on the insertion of nitrogen in RFMS carbon nitride films, *Diam. Relat. Mater.* 17 (2002) 700.
- [31] C. Wang, S. Yang, J. Zhang, Correlation between nitrogen incorporation and structural modification of hydrogenated carbon nitride films, *J. Non-Cryst. Solids* 354 (2008) 1608.
- [32] Y.H. Cheng, B.K. Tay, S.P. Lau, et al., Deposition of carbon nitride films by filtered cathodic vacuum arc combined with radio frequency ion beam source, *Diam. Relat. Mater.* 9 (2000) 2010–2018.
- [33] P. Hammer, F. Alvarez, Influence of chemical sputtering on the composition and bonding structure of carbon nitride films, *Thin Solid Films* 398 (2001) 116–123.
- [34] Z.B. Dong, Y.F. Lu, K. Gao, et al., Thermal stability of carbon nitride thin films prepared by electron cyclotron resonance plasma assisted pulsed laser deposition, *Thin Solid Films* 516 (2008) 8594.
- [35] D.W.M. Lau, A. Moafi, M.B. Taylor, et al., The structural phases of non-crystalline carbon prepared by physical vapour deposition, *Carbon* 47 (2009) 3263.
- [36] M. Moseler, P. Gumbsch, C. Casiraghi, et al., The ultrasmoothness of diamond-like carbon surfaces, *Science* 309 (2005) 1545–1548.
- [37] J. Ni, W. Wu, X. Ju, et al., Bonding structure of  $a\text{-CN}_x$ : H films obtained in methane-nitrogen system and its influence on hardness, *Thin Solid Films* 516 (2008) 7422–7426.
- [38] L. Yin, T.M. Shao, S.B. Wei, Preparation and characterisation of carbon nitride films deposited by pulsed laser arc deposition, *Int. J. Surf. Sci. Eng.* 4 (2010) 250–257.
- [39] O.S. Panwar, R.K. Tripathi, S. Chockalingam, Improved nanomechanical properties of hydrogenated tetrahedral amorphous carbon films measured with ultra low indentation load, *Mater. Express* 5 (2015) 410–418.
- [40] A.C. Fisher, Cripps: Nanoindentation, Springer, New York, 2004.
- [41] C.A. Charitidis, Nanomechanical and nanotribological properties of carbon-based thin films: a review, *Int. J. Refract. Met. Hard Mater.* 28 (2010) 51–70.